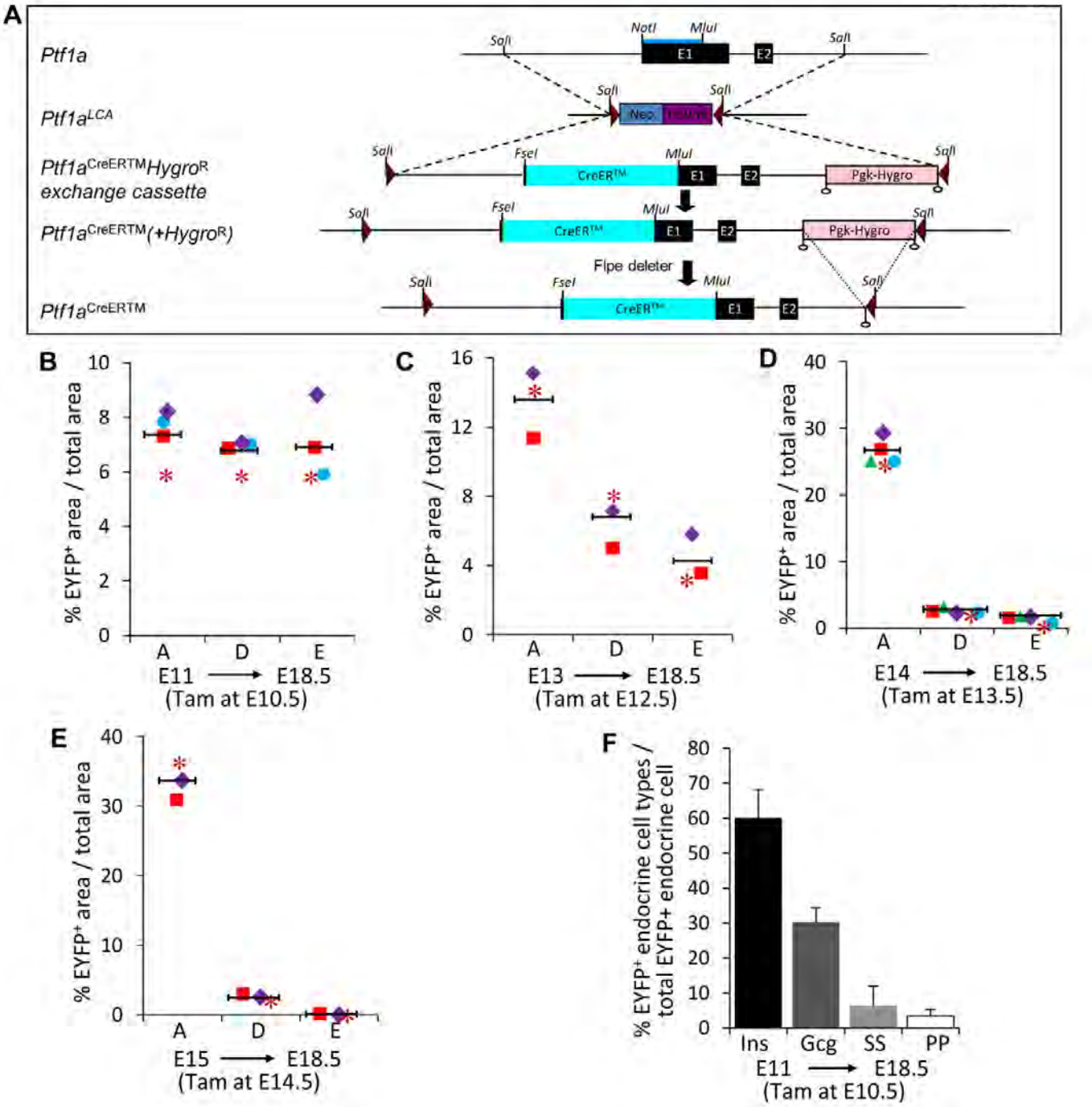

Fig. S1. Lineage tracing of *Ptf1a*-expressing cells using the novel *Ptf1a*^{CreERTM} allele. (A) Schematic representation of *Ptf1a*^{CreER} knock-in generation via recombinase-mediated cassette exchange (RMCE). A *Ptf1a*^{CreERTM}*Hygro*^{R}cassette exchange vector was constructed by inserting a 4105 bp fragment of *Ptf1a* into a plasmid containing two inversely oriented *LoxP* sites, and a 5′UTR *Not*I site was changed to *Fse*I. DNA encoding CreER^{TM} (a gift from Andrew McMahon, Harvard) was then inserted between this *Fse*I and a natural *Mlu*I site in *Ptf1a* exon 1. A *pgk*-driven *hygromycin* resistance gene (*Hygro*^{R}), flanked by tandem FRT sites, was inserted at the 3′ end of the exchange vector for positive selection during RMCE. RMCE was as previously described (Long et al., 2004). An embryonic stem (ES) cell clone 5D12 containing the *Ptf1a*^{LCA} (Burlison et al., 2008) was electroporated with the *Ptf1a*^{CreERTM}*Hygro*^{R} exchange vector and a Cre vector. Clones surviving hygromycin/gancyclovir selection were screened using PCR (primers sequences available upon request). Chimeric mice derived from injecting clone 5D12:1D7 ES cells into C57BL/6J blastocysts were bred with C57BL/6J mice to derive heterozygotes bearing *Ptf1a*^{CreERTM}*Hygro*^{R}. (B-E) The *HygroR* cassette was removed by *FLPe* deleter mice (provided by Susan Dymecki, Harvard). Scatter plots showing the percentage of cells in each pancreatic compartment expressing Eyfp after Tam injection at E10.5 (B; *n*=4), E12.5 (C; *n*=3), E13.5 (D; *n*=5), and E14.5 (E; *n*=3). Each point represents a single pancreas. (F) Ptf1a-expressing cells at E11 contribute equally to all endocrine cell types; *n*=3. A, acinar; D, duct; E, endocrine.

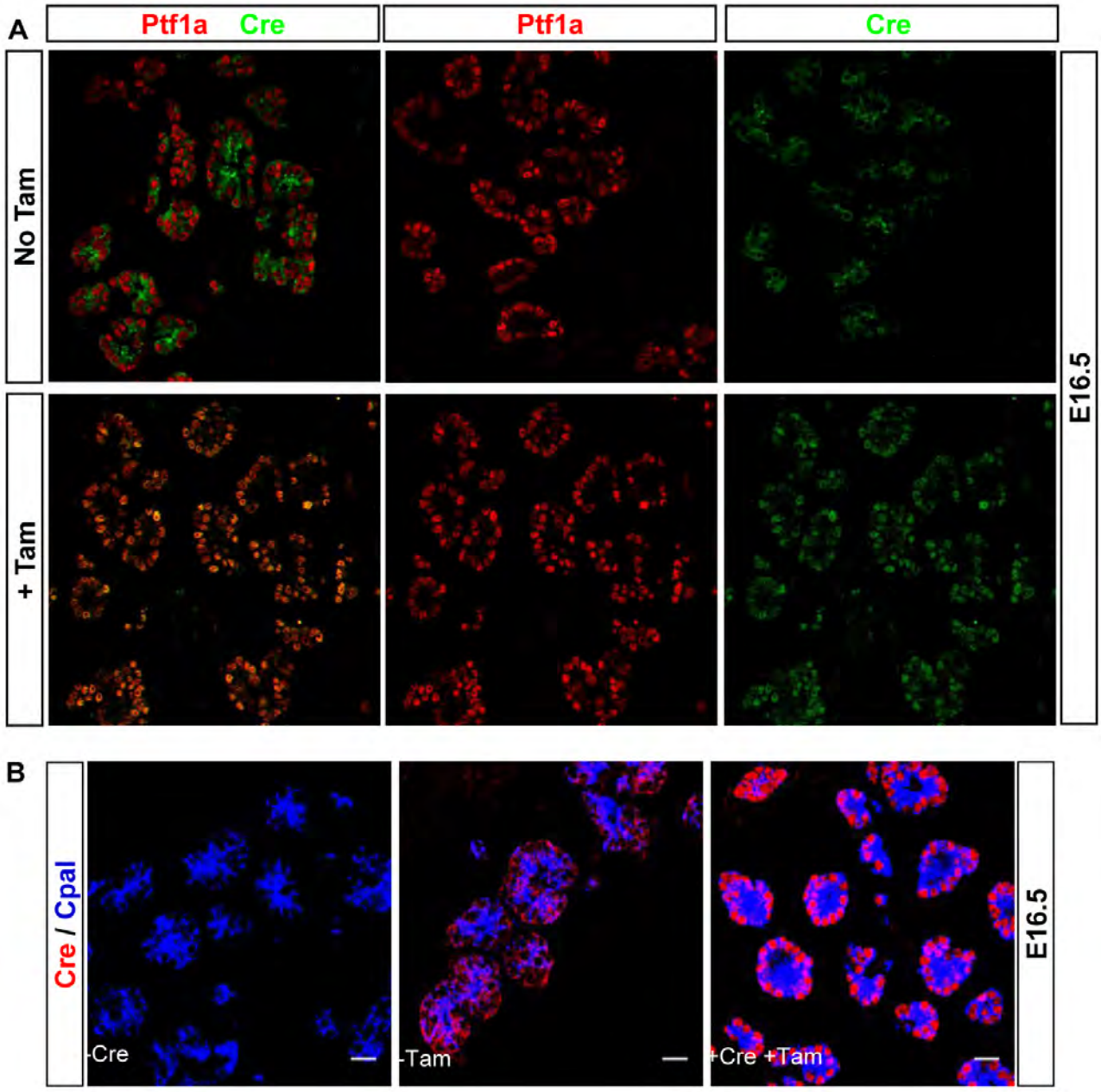

Fig. S2. Cre production recapitulate endogenous Ptf1a production. (**A**) Cre protein is located in the cytoplasm of Ptf1a^{+} cells in the absence of tamoxifen at E16.5 (upper panel); tamoxifen treatment resulted in nuclear translocation of Cre in Ptf1a^{+} cells (lower panel). (**B**) Cre protein was not detected in wild-type E16.5 CpaI^{+} cells, and tamoxifen treatment caused nuclear localization of Cre in CpaI^{+} cells. Scale bar: 50 μm.

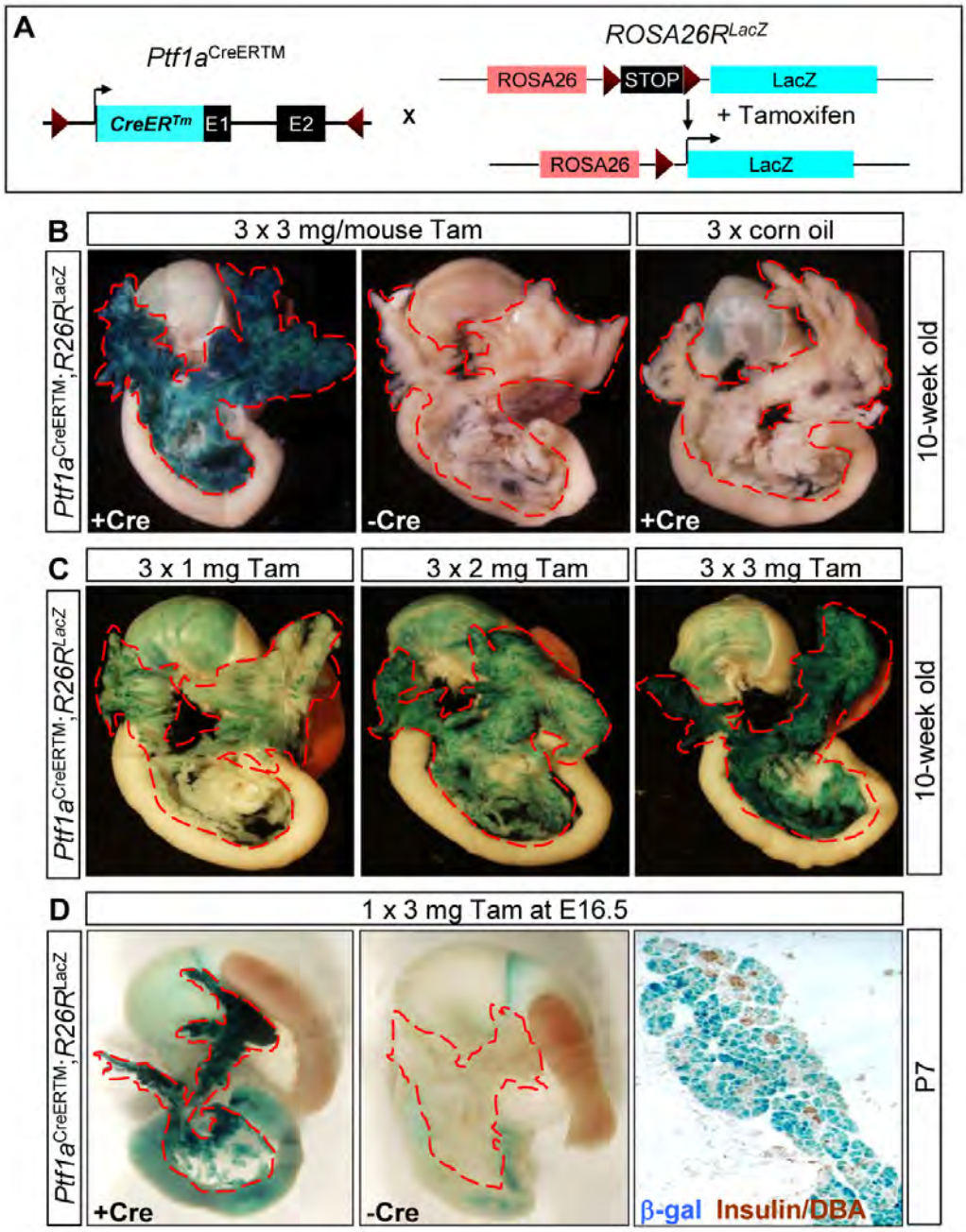

Fig. S3. *Ptf1a*$^{\text{CreERTM}}$-induced recombination at the *ROSA26R*$^{\text{lacZ}}$ allele is Tam and Tam-dosage dependent. (**A**) Schematic presentation of *Ptf1a*$^{\text{CreER}}$-mediated recombination at the *Rosa26*$^{\text{Eyfp}}$ locus only in the presence of Tam. (**B**) Whole-mount β-gal-stained adult gut tissues showed that β-gal staining was found in the pancreas only in the presence of Tam (left panel), but not in corn-oil injected control (right panel), indicating the absence of leakiness. (**C**) There was a Tam-dosage-dependent increase (from 3 to 9 mg) in the β-gal^{+} cell numbers in the pancreas. (**D**) Efficient embryonic labeling at E16.5 after a single dose 3 mg Tam injection (left panel). β-gal staining was mainly found in acinar cells. β-gal staining was not found in the pancreas of mice that did not carry the *Ptf1a*$^{\text{CreERTM}}$ allele (B, middle panel; D, middle panel).

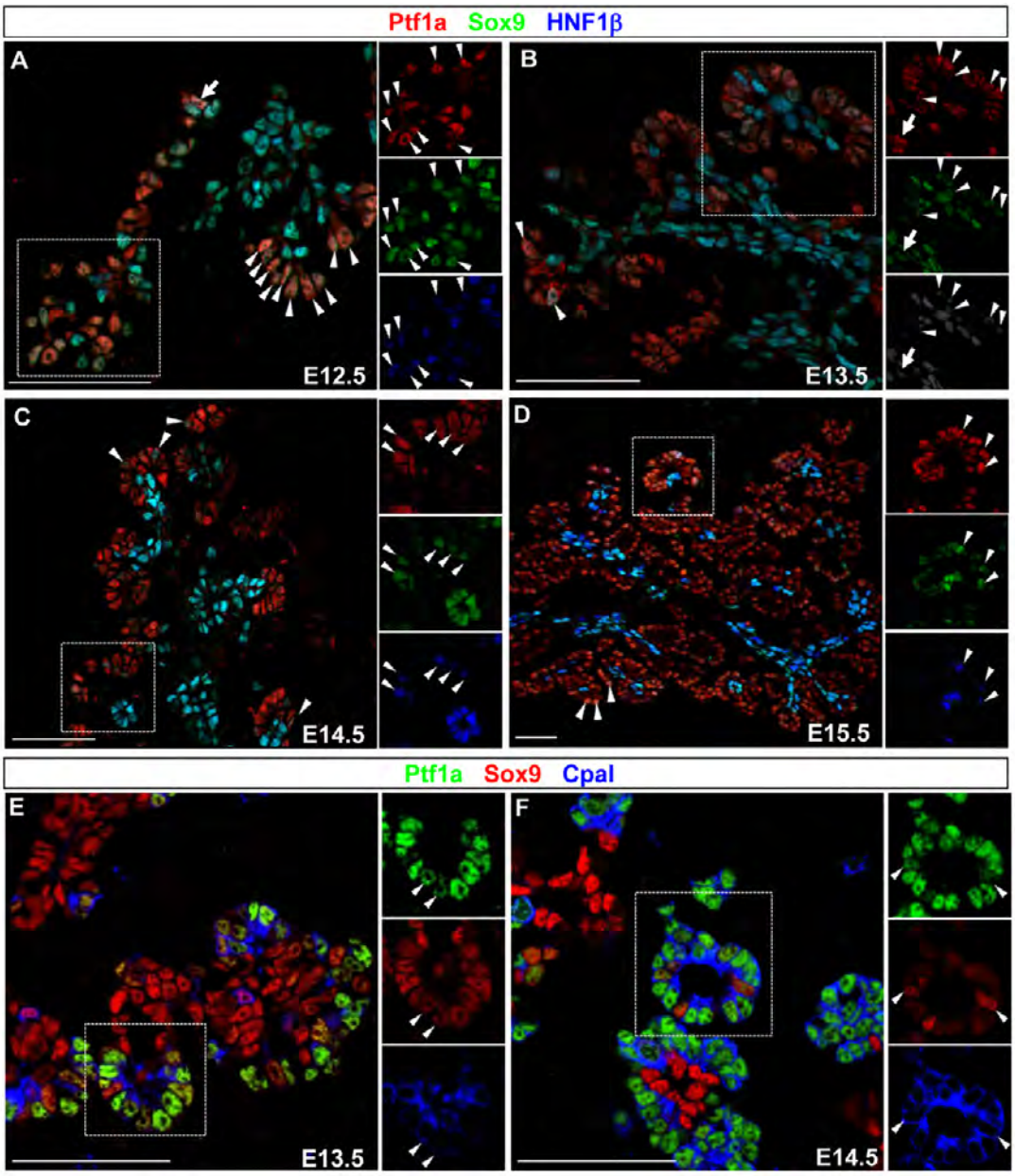

Fig. S4. Distribution of Ptf1a^{+}Sox9^{+}Hnf1β^{+} tip MPCs during the 2° transition. Immunolabeling analysis of Ptf1a, Sox9 and Hnf1β at (**A**) E12.5, (**B**) E13.5, (**C**) E14.5 and (**D**) E15.5 shows the distribution and decreasing numbers of Ptf1a^{+}Sox9^{+}Hnf1β^{+} tip MPCs (arrowhead and arrow) in both intra-tip and tip-trunk interface region. A definite intra-tip location is defined by the location at or near the most distal tip region of the pancreatic epithelium, contact with adjacent pancreatic mesenchyme, and importantly the absence of any cells positive for trunk markers (Sox9^{HI}Hnf1β^{+}) next to that cell's location, from analysis of all of the adjacent sections (arrowhead). 'Tip MPCs' that are located at the tip-trunk interface are defined by proximity to the Sox9^{HI}Hnf1β^{+} trunk cells (arrow). The Ptf1a^{+}Sox9^{+} tip MPCs are also CpaI^{+} (arrowhead) at (**E**) E13.5 and (**F**) E14.5. Scale bar: 50 μm.

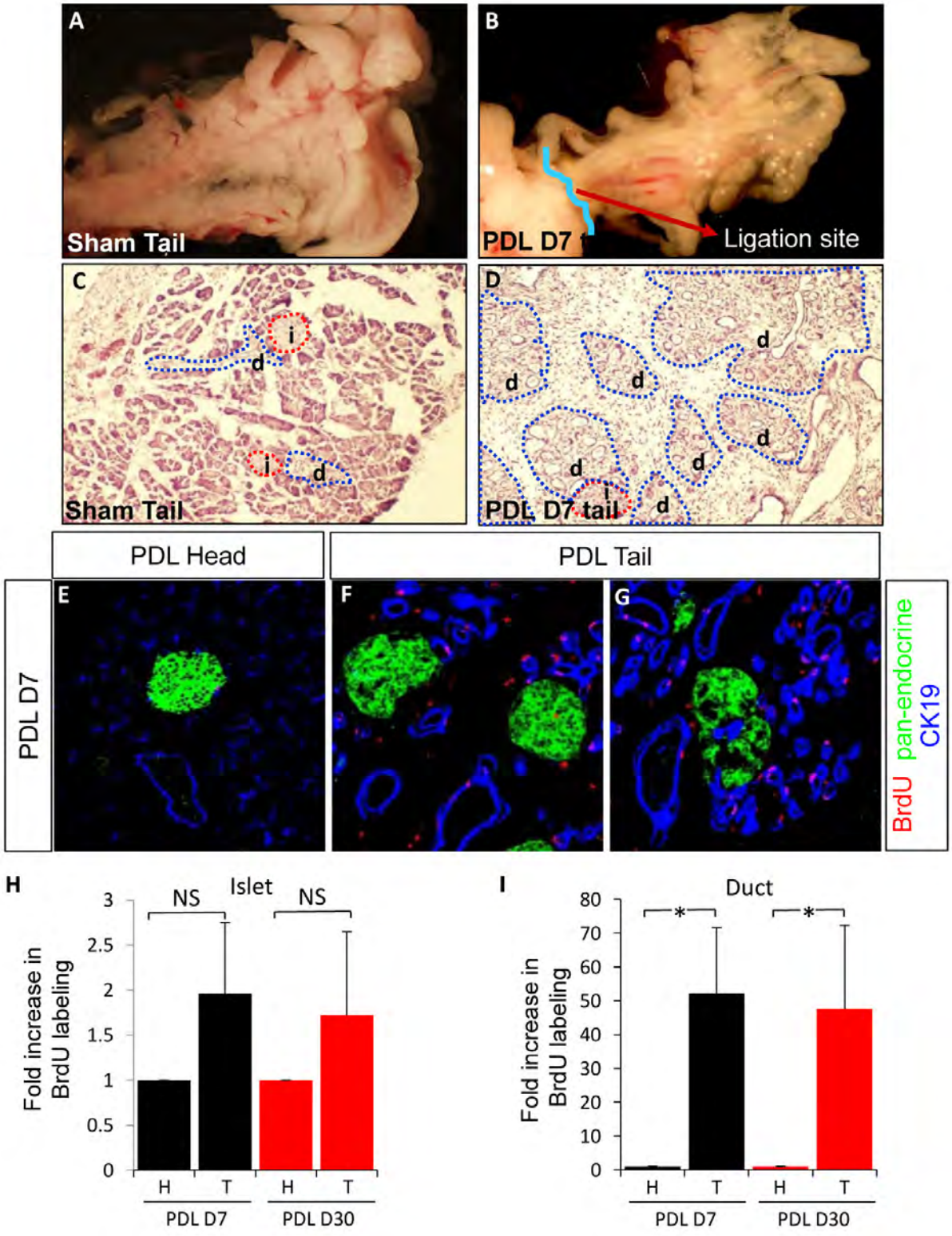

Fig. S5. PDL induces dramatic increased in proliferation in the remodeling ducts. (**A**,**B**) Gross morphological appearance of PDL tail at post-PDL D7 (B) compared to sham tail (A). (**C**,**D**) Sections of sham tail (C) and PDL tail (D) stained with Hematoxylin and Eosin (H&E). (**E-I**) Significant increased BrdU incorporation in the ducts of PDL D7 and D30 tail (F,G,I) compared with PDL head (E,I) indicate active proliferation of remodeling ducts. No significant changes in BrdU labeling in islet cells between PDL head and tail tissues (H). *P<0.005. d, ducts; I, islet; NS, not significant.

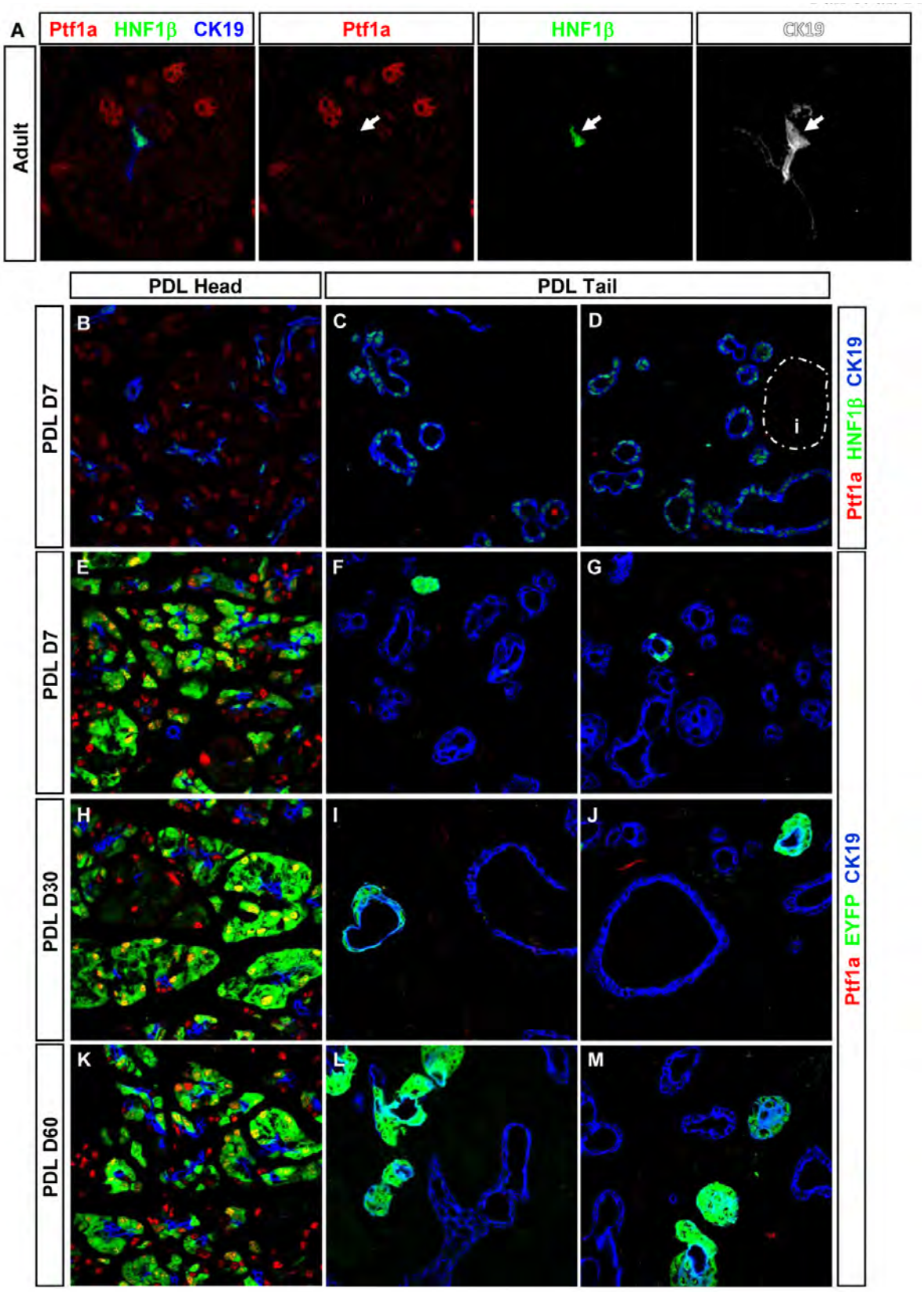

Fig. S6. Ptf1a production in mature adult pancreas and PDL-injured pancreas. (**A**) Ptf1a protein is not detected in Hnf1β^{+}Ck19^{+} CACs. Ptf1a protein is only detected in acinar cells, but not in Hnf1β^{+}Ck19^{+} duct cells in both PDL head and tail tissues at PDL (**B-G**) D7, (**H-J**) D30 and (**K-M**) D60. i, islet.

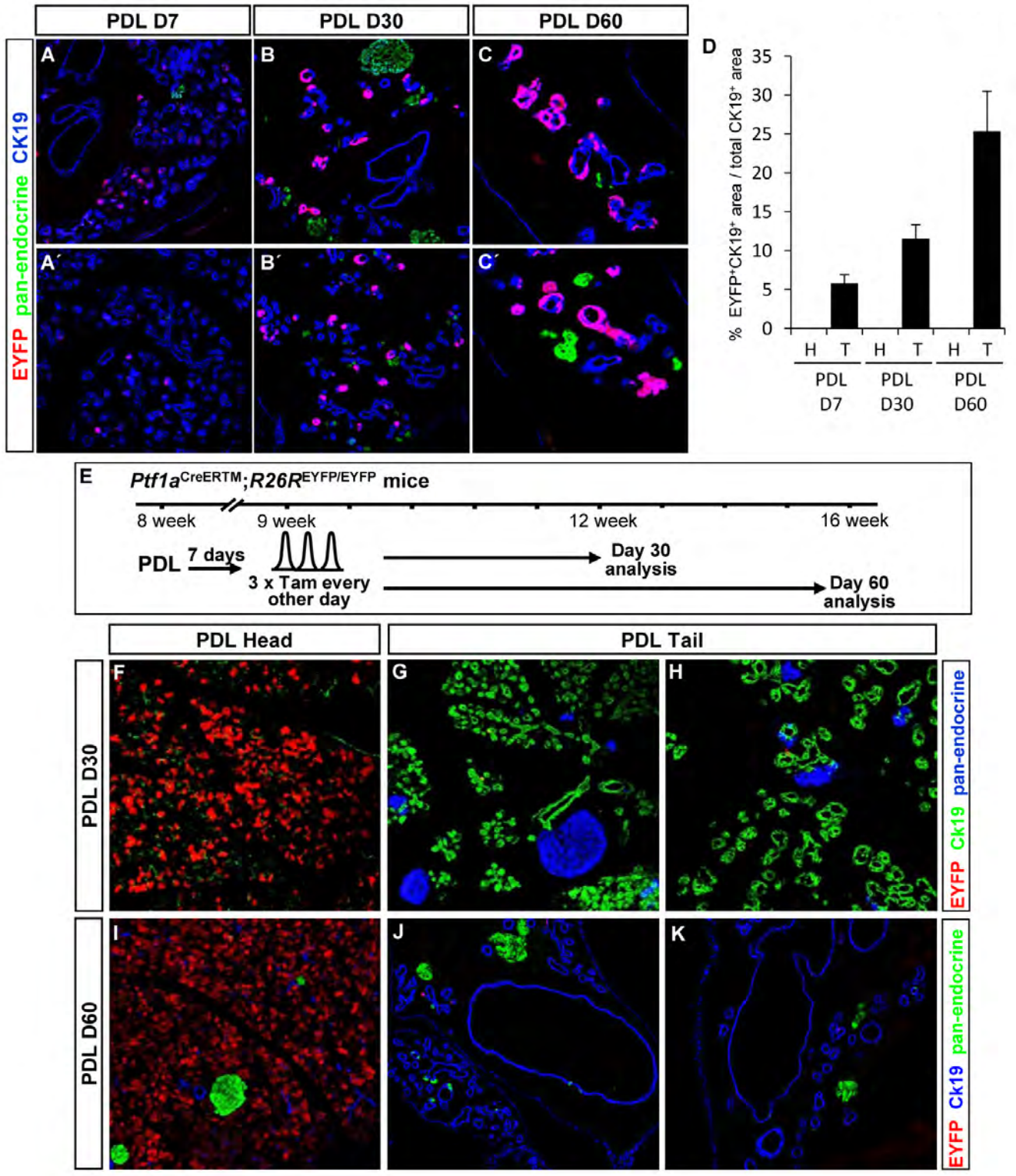

Fig. S7. *Ptf1a* lineage-labeled duct cells were derived from acinar-to-ductal transdifferentiation, and not direct activation of *Ptf1a* expression in the ducts post-PDL. (**A-C′**) *Ptf1a*-lineage labeled (Eyfp^{+}Ck19^{+}) ducts in PDL tail at PDL (A,A′) D7, (B,B′) D30, and (C,C′) D60. (**D**) Quantitation analysis of percentage of Ptf1a-derived duct cells over total Ck19^{+} duct cells. (**E**) Schematic of post-PDL tamoxifen-treatment lineage-tracing analysis. Labeling efficiency in acinar cells remained high in PDL head tissue when tamoxifen was administrated post PDL at PDL (**F**) D30 and (**I**) D60. Very rare *Ptf1a*-derived Ck19^{+} duct cells were found at PDL (**G**,**H**) D30 and (**J**,**K**) D60 when tamoxifen was injected at post-PDL D7.

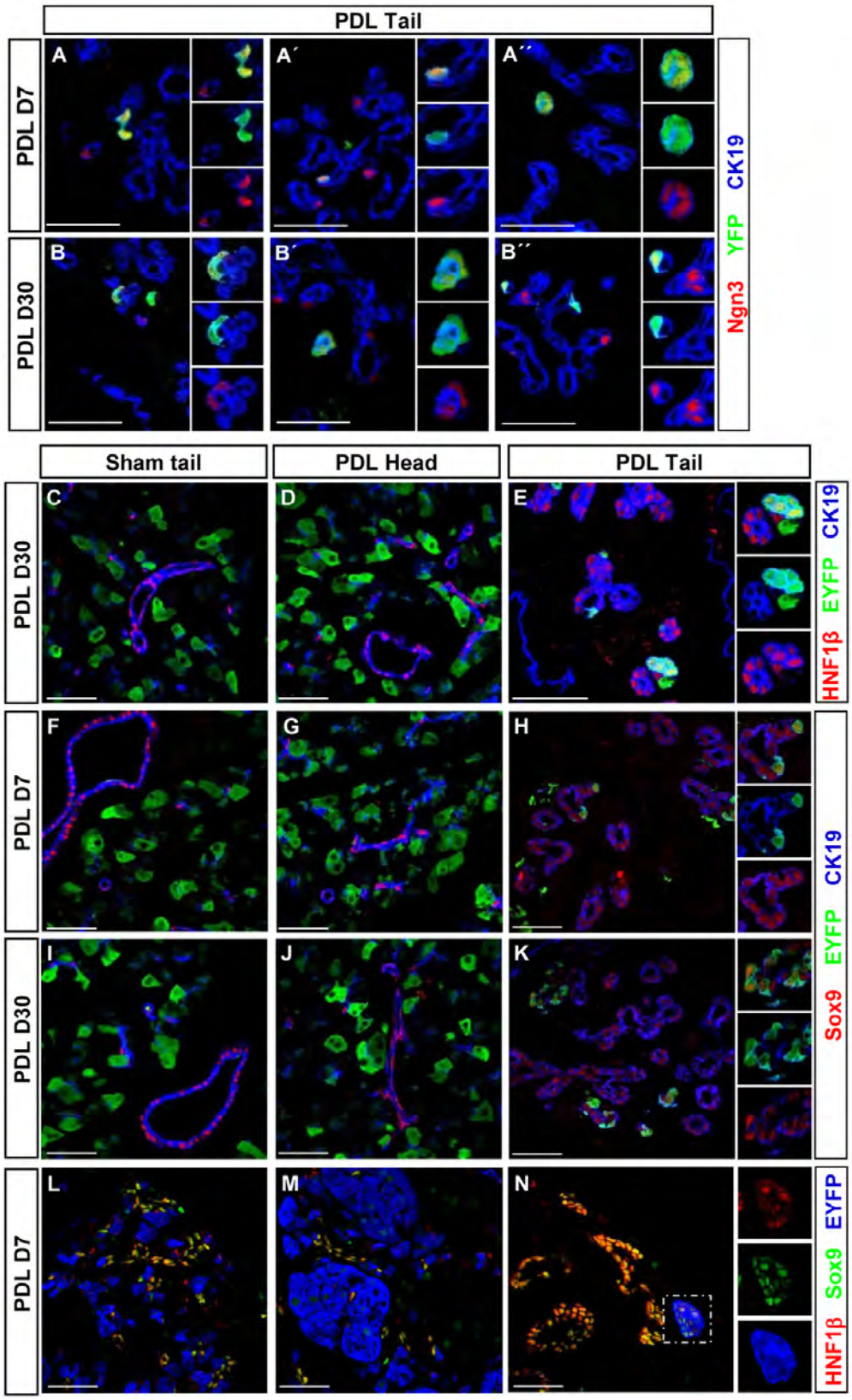

Fig. S8. PDL induces acinar-to-ductal transdifferentiation and activates of Ngn3 protein production in duct cells. (**A-B′**) Additional examples of Ptf1a-lineage-labeled Ngn3^{+}Ck19^{+} duct cells at post-PDL D7 (A-A′) and D30 (B-B′). (**C-N**) Ptf1a^{+} acini gave rise to long-lived Hnf1β^{+} (E) and Sox9^{+} (H,K) duct cells in PDL tail at post-PDL D7 and D30, but not in sham tail (C,F,I) or PDL head (D,G,J). The Sox9^{+}Hnf1β^{+} duct cells are Eyfp^{-} in sham tail (L) or PDL head (M). Most of the Ptf1a^{+} acinar-derived duct cells at PDL D7 are Sox9^{+}Hnf1β^{+} (N). Scale bar: 50 μm.

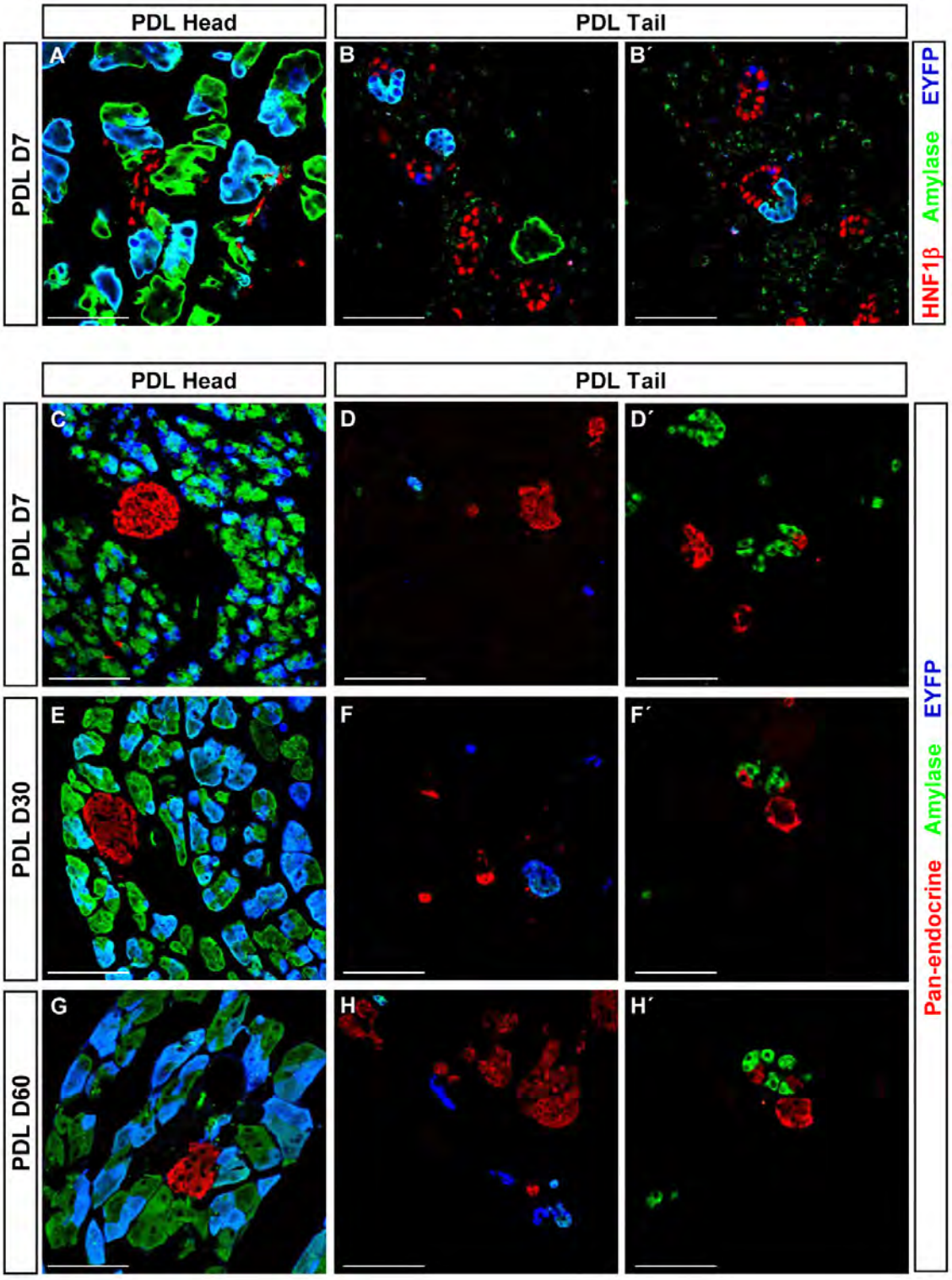

Fig. S9. PDL did not induce direct acinar-to-endocrine transdifferentiation. (**A-B′**) Hnf1β^{+} duct cells did not express amylase at PDL D7 in both head (A) and tail (B,B′), suggesting that acinar enzymes were downregulated before the activation of multipotency factors, such as Hnf1β. (**C-H′**) Amylase was only found in acini in PDL head at PDL D7 (C), D30 (E) and D60 (G). No Amylase^{+}hormone^{+} transitional cell state was found in PDL tail post-PDL D7 (D,D′), D30 (F,F′) and D60 (H,H′), suggesting that Ptf1a-lineage-derived endocrine cells are not a result of rapid, direct acinar transdifferentiation, but stepwise acinar-to-duct-to-endocrine reprogramming.

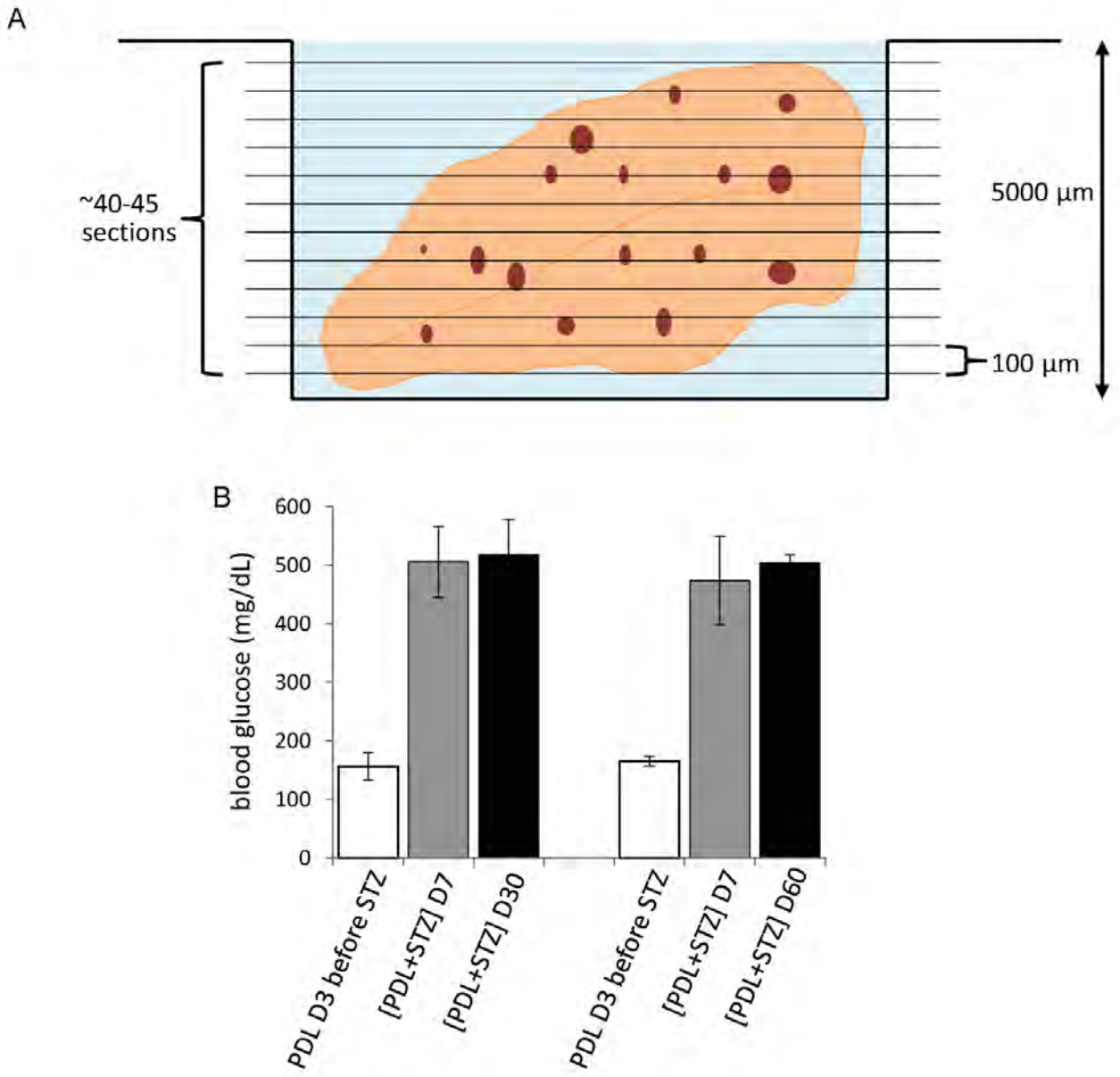

Fig. S10. Strategy for tissue collection and quantitation analysis. Sham tail and PDL tail were embedded in OCT for cryosectioning. (**A**) The whole tissue block was sectioned, we examined ~40-45 sections, taken at 100 µm distance, and stained with a cocktail of endocrine hormones (including insulin, glucagon, somatostatin and pancreatic polypeptide). The pictures were taken at 10´ magnification to include all the hormone$^+$ areas. The islet areas were measured using NIH ImageJ (v. 1.4.3.76) software. (**B**) PDL+STZ treated mice remained hyperglycemic at PDL+STZ D30 and D60. While there is a significant increase in Ptf1a-lineage-derived insulin$^+$ β-cells, the small number of β-cells generated in this transdifferentiation process is therefore insufficient to improve overall glucose homeostasis.

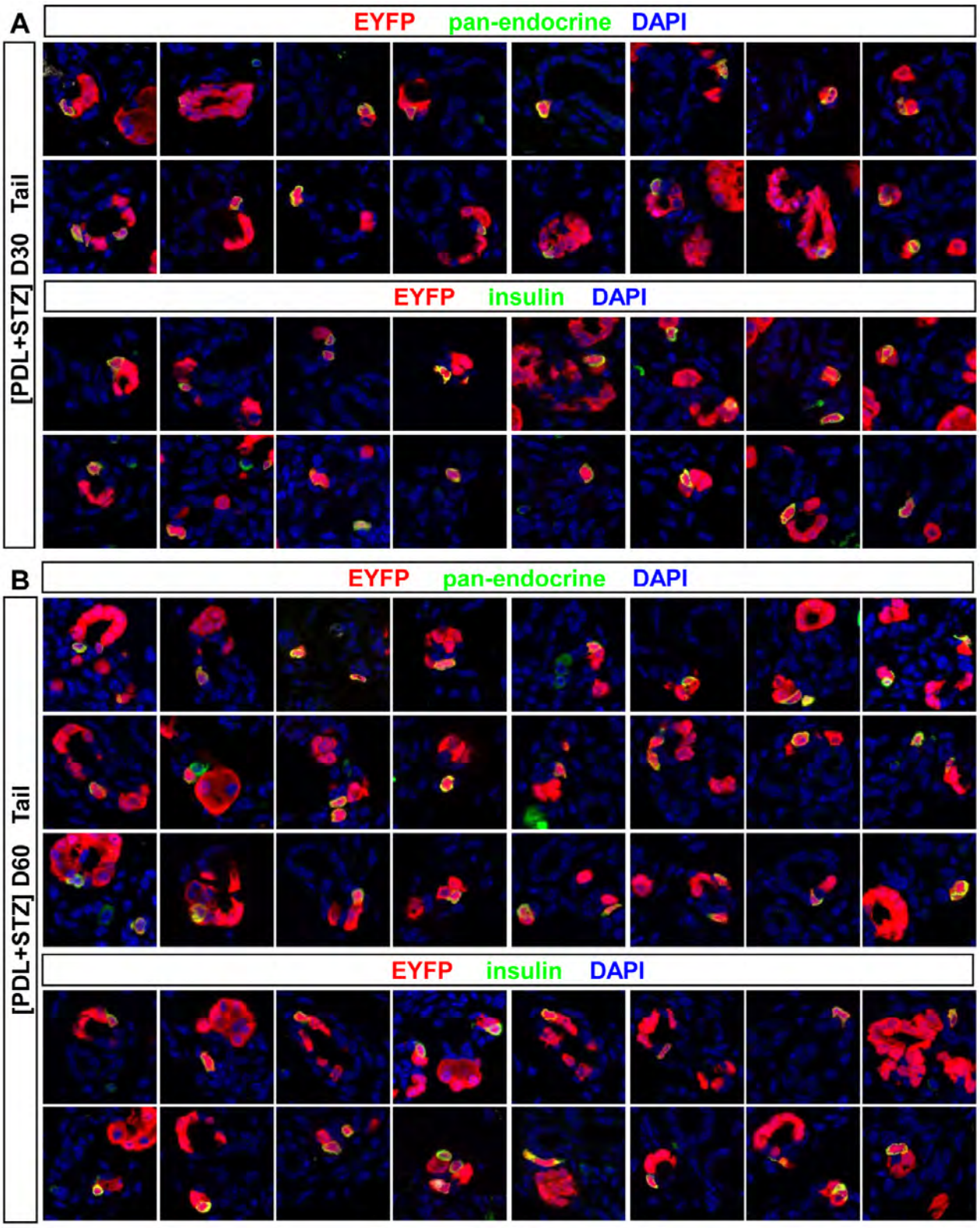

Fig. S11. *Ptf1a* lineage-labeled endocrine/β-cells. Additional examples of *Ptf1a*-lineage-labeled endocrine-hormone$^+$ cells (upper panel) and insulin$^+$ cells (lower panel) at [PDL+STZ] D30 (**A**) and [PDL+STZ] D60 (**B**).

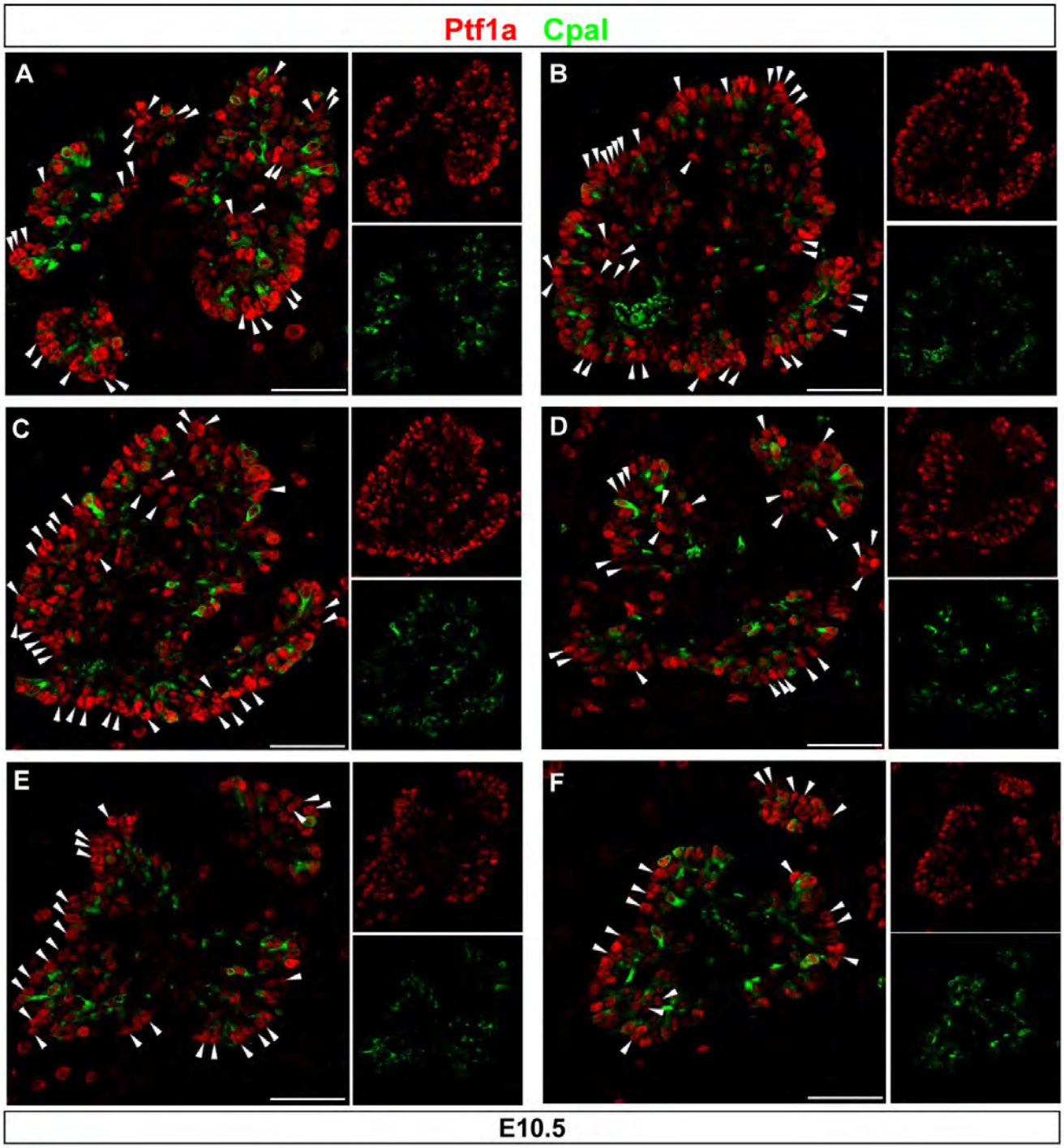

Fig. S12. Numerous Ptf1a^{+} cells do not co-express CpaI at E10.5. (**A-F**) Immunolabeling analysis of Ptf1a and CpaI from different regions of E10.5 dorsal pancreas bud shows that the Ptf1a^{+}CpaI^{-} cells (arrowhead) were frequently found at this stage, suggesting CpaI may only marks a fraction of MPC populations. Scale bar: 50 μm.

Table S1. Antibodies

Primary antibodies				
Antigen	**Species**	**Dilution**	**Staining type**	**Source**
Ptf1a	Rabbit	1:1000	TSA	BCBC
Ptf1a	Guinea pig	1:500	IF	Jane Johnson (UTSW)
Hnf1β	Goat	1:500	TSA	Santa Cruz
Sox9	Rabbit	1:1000	IF	Chemicon
Ngn3	Guinea Pig	1:2000	TSA	M. Sander (UCSD)
GFP	Rabbit	1:500 1:1000	IF TSA	Clontech
GFP	Chicken	1:500	IF	Aves
Insulin	Guinea Pig	1:1000	IF	Linco
Insulin-A	Goat	1:250	IF	Santa Cruz
Glucagon	Guinea Pig	1:1000	IF	Linco
Glucagon	Rabbit	1:1000	IF	Linco
Somatostatin	Goat	1:1000	IF	Santa Cruz
Pancreatic polypeptide	Guinea Pig	1:1000	IF	Linco
CpaI	Goat	1:250	IF	BD Bioscience
E-cadherin	Mouse	1:500	IF	BD Bioscience
BrdU	Mouse	1:500	IF	BD Pharmingen
Ck19	Rabbit	1:2000	IF	B. Stanger (U. Penn)
Dba	Biotinylated	1:250	IF	Vector Laboratories
Synaptophysin	Rabbit	1:1000	TSA	DakoCytomation
Cre	Guinea Pig	1:2000	TSA	C. Wright (Vanderbilt)

Secondary antibodies			
Antigen	**Conjugation**	**Dilution**	**Source**
Rabbit/guinea pig/ goat/mouse/chicken	Cy3	1:300	Jackson ImmunoResearch
Rabbit/guinea pig/ goat/mouse/chicken	Cy2	1:300	Jackson ImmunoResearch
Rabbit/guinea pig/goat/mouse	Cy5	1:300	Jackson ImmunoResearch
Rabbit/guinea pig/ goat/mouse/chicken	Biotinylated	1:1000	Vector Laboratories